The olfactory gating of visual preferences to human skin and colors in mosquitoes

Diego Alonso San Alberto[1,2], Claire Rusch[1,2], Yinpeng Zhan[3], Andrew D. Straw[4], Craig Montell[3], and Jeffrey A. Riffell[1,†]

[1]Department of Biology, University of Washington, Seattle, WA 98195, USA,

[2]Both authors contributed equally,

[3]University of California, Santa Barbara, Santa Barbara CA 93106, USA,

[4]Institute of Biology I & Bernstein Center Freibug, Albert-Ludwigs-Univesität Freiburg, Germany

Keywords: color vision, olfaction, sensory integration, mosquitoes, *Aedes aegypti*

---

*Lead contact and to whom all correspondence should be addressed:

Jeffrey A. Riffell

Department of Biology,

University of Washington,

Seattle, WA 98195, USA

e-mail: jriffell@uw.edu

Abstract

Mosquitoes track odors, locate hosts, and find mates visually. The color of a food resource, such as a flower or warm-blooded host, can be dominated by long wavelengths of the visible light spectrum (green to red for humans) and is likely important for object recognition and localization. However, little is known about the hues that attract mosquitoes or how odor affects mosquito visual search behaviors. We used a real-time 3D tracking system and wind tunnel that allowed careful control of the olfactory and visual environment to quantify the behavior of more than 1.3 million mosquito trajectories. We found that CO_2 induces a strong attraction to specific hues, including those that humans perceive as cyan, orange, and red. Sensitivity to orange and red correlates with mosquitoes' strong attraction to the color spectrum of human skin, which is dominated by these wavelengths. Attraction was eliminated by filtering the orange and red bands from the skin color spectrum and by introducing mutations targeting specific long-wavelength opsins or CO_2 detection. Collectively, our results show that odor is critical for mosquitoes' wavelength preferences and that the mosquito visual system is a promising target for inhibiting their attraction to human hosts.

Introduction

The behavioral preference of insects for certain bands in the visible light spectrum plays a profound role in structuring ecological communities by mediating processes such as plant-insect/predator-prey interactions and disease transmission[1-3]. For biting insects, such as mosquitoes, tsetse flies, and kissing bugs, vision plays an essential role in various behaviors, including flight control, object tracking for host- or nectar-finding, and locating oviposition sites[4]. The visual stimuli that mediate these behaviors are integrally tied to other host-related cues, such as scent and heat. For instance, when combined with an odor lure, tsetse flies are highly attracted to what humans perceive as blue color[5,6], and kissing bugs prefer visual objects only when also associated with odors[7]. Visually guided mosquito behaviors are also thought to play a role in host attraction[8-10]. It has long been known that mosquitoes are attracted to dark, high-contrast objects[9,11], which has led to the development of black traps[10]. For high-contrast visual stimuli, recent work has shown that certain odors stimulate visual search behaviors in *Aedes aegypti* mosquitoes. This species is not attracted to black objects in the absence of CO_2, but after encountering a CO_2 plume, they become highly attracted to such objects[11]. Other cues (heat, water vapor, skin volatiles) mediate behaviors such as landing and biting[11-14].

Despite the potential importance of color in mediating mosquito biting behaviors, surprisingly, details regarding other wavelengths that attract mosquitoes or how odors sensitize that attraction remain

unclear. The visual spectra of important resources can be diverse and dominated by short and medium wavelengths (e.g., flowers or oviposition sites) or long wavelengths (e.g., human skin) (Fig. 1A, B). Despite interest in developing traps and lures that exploit mosquito spectral preferences, only a few studies have examined these preferences, and the results of those studies have been contradictory. For instance, studies of *Ae. aegypti* have shown no difference in spectral preference in the 450–600 nm wavelength range[15,16]. By contrast, other studies have demonstrated specific preferences but for different wavelength bands: *Ae. aegypti* mosquitoes were attracted to blue in one study[17] and only to green-yellow in another[18]. Other studies have shown that mosquitoes sometimes prefer red[15,19,20], although it is thought that mosquitoes lack opsin receptors sensitive to these wavelengths. Because mosquitoes are attracted to dark visual objects, responses to red may represent achromatic responses from visual channels that are sensitive to medium-wavelengths and therefore are perceived as dark grey or black when presented against a light-colored background. Nevertheless, these prior studies did not characterize the actual flight trajectories of the mosquitoes, nor control for the change in behavioral state associated with the smell of a host. Accurate control of both a visual object's reflectance and its contrast with the background is required to determine whether mosquitoes are attracted to specific wavelengths.

Aedes aegypti provides an excellent model for studies aimed at elucidating spectral preferences and determining how these preferences are modulated by odor. *Aedes aegypti*, which are active during the dawn and dusk periods[21], have 10 rhodopsins, 5 of which are expressed in the adult eye[22]. Little is known about opsin tuning, although they are orthologs of medium-wavelength sensitive opsins (green), and previous electroretinogram (ERG) studies suggested that *Ae. aegypti* is sensitive to medium-long wavelengths in the green-yellow spectrum[23, 24]. In this study, we used a large wind tunnel and computerized vision system to close these knowledge gaps regarding mosquito visual and olfactory responses by examining *Ae. aegypti* free-flight responses to objects of different wavelengths, with and without the presence of CO_2. We show that when experiencing odor, mosquitoes become particularly attracted to hues that are dominant in human skin. We also demonstrate that knockout of either the olfactory channel that gates visual attraction or the opsins that allow detection of objects that reflect long wavelengths eliminates attraction to skin tones.

Results

Olfactory gating of spectral preferences of Ae. aegypti mosquitoes

Examining olfactory and visual search behaviors in mosquitoes often requires simulating conditions in which the statistics of the stimuli (e.g., intensity, duration) and resulting mosquito behavior are as natural as possible. We therefore examined *Ae. aegypti* behavior in a large wind tunnel spanning 450 mosquito

body lengths and equipped with a 16-camera, real-time tracking system for monitoring and quantifying mosquito behaviors[11,25]. A checkerboard pattern was projected on the bottom (floor) of the wind tunnel, and a low-contrast grey horizon was projected on each side of the tunnel to provide optic flow (Fig. 1C). Similar to our previous assays, we placed two identically sized circles (3-cm diameter) on the floor of the tunnel in the upwind area of the working section, 18 cm apart and 33 cm from the odor source (Fig. 1C). In each experimental trial, 50 mated *Ae. aegypti* females were released into the tunnel, and their trajectories were recorded over a 3-h period (1.3 million total trajectories were recorded, with an average trajectory duration of 3 s). The tunnel was filled with filtered air for 1 h, after which a CO_2 plume (95% filtered air, 5% CO_2) located 33 cm away and separate from the visual objects was introduced into the tunnel and left for 1 h (Fig. 1D). Measurements of the plume showed an exponential decay, typical of turbulent diffusion, with a concentration of ~1500 ppm approximately 30 cm from the odor source. In the last hour of the experiment, only filtered air was released into the wind tunnel.

During exposure to filtered air, the mosquitoes exhibited random behavior to the odor source and visual objects, and they spent much of their time exploring the ceiling and walls of the tunnel and rarely investigated the visual objects (Fig. 1F). By contrast, upon exposure to the CO_2 plume, the number of flying mosquitoes more than doubled (Fig. 1F, H; Wilcoxon signed-rank test, number of trajectories in Air vs. CO_2, $P < 0.002$). During this time, the mosquitoes exhibited odor-tracking behavior, spending most of the time in the working section's central area with significantly elevated flight velocities (Figs. 1F, S1; Kruskal-Wallis test: df = 2, Chi-square = 597.23, $P < 0.0001$). The CO_2 also triggered an attraction to the visual objects. The mosquitoes showed no interest in the objects during the filtered air treatment (only 1–4% of mosquitoes investigated), but during CO_2 release, the percentage and number of mosquitoes investigating the visual objects increased significantly (21%; paired Student's t-test, $P = 0.002$) (Fig. S1E). After the plume was stopped, the attraction to the visual objects ceased (Fig. 1E, S1F, Wilcoxon signed-rank test, CO_2 vs. Post-CO_2: $P < 0.001$).

To ensure that mosquito visual preference behaviors were in response to discrete wavelength bands rather than object contrast, we employed visual stimuli in the range 430 to 660 nm (violet to red to a human observer; hereafter, visual stimuli are referred to as they are perceived by the human eye without implying that mosquitoes have the same subjective experience of color), with each visual stimulus having the same approximate contrast with the background (Fig. 1G). While investigating the visual objects, the mosquitoes would fly upwind and hover immediately downwind of a visual object, at approximately 3–5 cm, while exhibiting brief excursions before returning to the objects (Fig. 1E). During CO_2 release, the same total number of mosquitoes was recruited to the visual objects of differing hues (Fig. S1E). Relative to the white control object, however, the mosquitoes preferred certain hues, such as cyan, red, and orange,

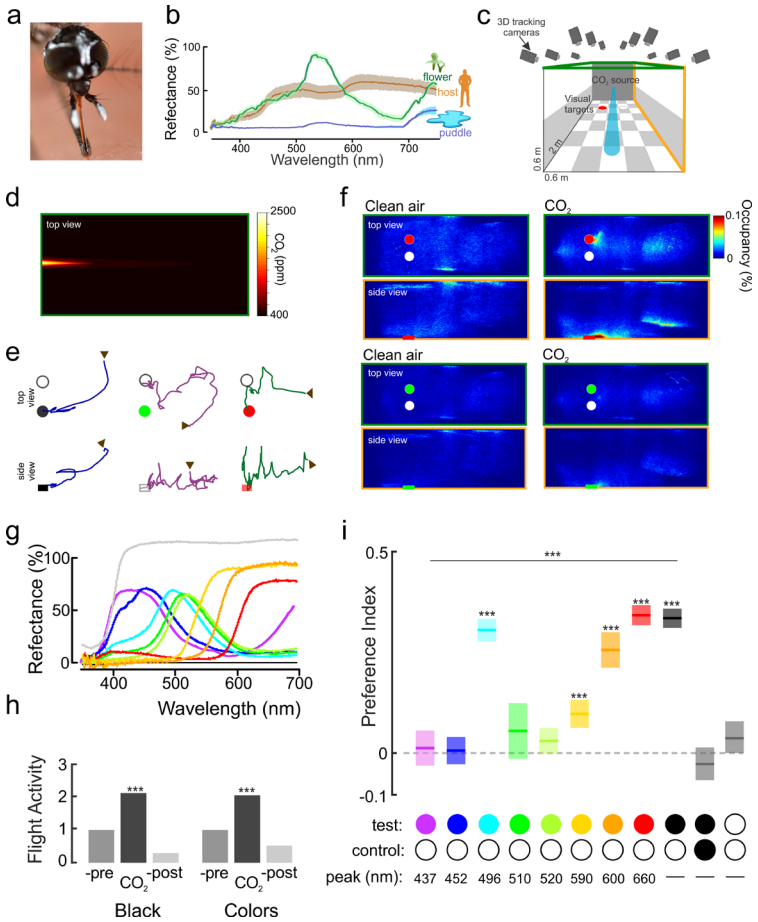

Figure 1. Olfactory gating of mosquito color preference. (**A**) The *Ae. aegypti* eye. The retina is composed of ~300-400 ommatidia and ranges in spectral sensitivity from the near-ultraviolet (300 nm) to orange-red (600-700 nm) wavelengths. Image courtesy of Raúl Pardo (with permission). (**B**) Spectral reflectance of behaviorally important objects for *Ae. aegypti* females: human skin (brown line); flower (*P. obtusata*; green line) and small puddle filled with *Ae. aegypti* larvae (blue line). (**C**) Wind tunnel system with real-time tracking system, odor and visual stimulation. (**D**) Heat map of the CO_2 plume in the wind tunnel. (**E**) Example of individual trajectories (top: [x-,y-axes], bottom: side view [x-,z-axes]). The arrows represent the start of a trajectory and the circles are the visual objects. (**F**) Heat (occupancy) maps showing the distribution of female mosquitoes without (left panels) and with CO_2 delivery (right panels) while in presence of a white and a red objects (top), or white and green objects (bottom). The position of the plots shows the top and side views of the tunnel working section. (**G**) Reflectance of the visual stimuli used in the experiments. (**H**) Relative flight activity between the different phases of the experiments (pre-, CO_2 and post-CO_2) as the number of trajectories recorded during one phase divided by the number of trajectories recorded in the previous phase. There were no significant differences in the relative activity during the CO_2 phase when the tested visual object was black versus objects of different hues (Kruskal-Wallis test, df = 1, Chi-sq = 0.01, P = 0.92). (**I**) Mean preference index for the test object (black, or different hues) vs. the control (white) object. There was a significant effect of hue on the attraction to the tested object (Kruskal-Wallis test, Preference index ~ pair of visual stimuli used, df = 8, Chi-sq = 597.23, P < 0.0001). Several hues were significantly more attractive than the control, white object (one-sample t-test: ***: P < 0.001). Boxplots area the mean (line) with 95% confidence interval (shaded area) (n ≥ 17,729 mosquito trajectories for each tested object).

as demonstrated by their focused clustering around the object (Fig. 1E). By contrast, other hues (violet, blue, green, and green-yellow) elicited no attraction responses compared to the white object (Fig. 1E, I). Across all hues, CO_2 had a strong effect on flight velocity and duration, but there were no significant differences between treatments (Fig. S1B, D) (Kruskal-Wallis test: Chi-square < 16.82, P > 0.11), demonstrating that the presence of CO_2 is necessary for attraction to specific hues and that visual preference did not result from higher flight velocity increasing the probability of a mosquito randomly encountering a visual object.

To further investigate mosquito spectral preferences, a preference index value (defined as the time spent investigating a colored object minus the time investigating the white object, divided by the sum of the times spent investigating the colored and white objects) was calculated for each mosquito that investigated a visual object. The hues differed significantly in terms of mosquito preference (Fig. 1I, Kruskal-Wallis test: df = 8, Chi-square = 597.23, $P < 0.0001$); several hues were more attractive to mosquitoes than the white object that served as a non-attracting control (Fig. 1I, one-sample t-test: $P < 0.001$). As the hues transitioned from green to red, the attractiveness of the object also increased. For instance, orange and red visual objects were strongly preferred by female mosquitoes (multiple comparison Kruskal-Wallis test: $P < 0.05$), whereas green, blue, and violet objects were not more attractive than the white control object (Kruskal-Wallis test: $P > 0.05$). However, mosquitoes were not restrictly attracted to the longest wavelengths, as they were also significantly attracted to cyan objects (peak reflectance at 496 nm). As a control to test for the effect of visual object attraction relative to other regions of the working section, we examined the preference between the white (control) object and a randomly selected volume in the wind tunnel. Compared with the randomly selected volume, female mosquitoes investigated the white object significantly more in presence of CO_2 (preference index = -0.53 ± 0.03 (mean ± sem), one-sample t-test: $P < 0.001$).

Behavioral preferences for orange-red wavelengths reflected from human skin

Across all skin tones, human skin has a strong signature in the long wavelength range (yellow, red) (Fig. 2A)[26], but it is unclear which bands in the human skin spectrum are most attractive to mosquitoes. To examine whether mosquitoes exhibit different preferences for certain spectral bands reflected by human skin, we first utilized color cards designed for cosmetics purposes to match human skin tones (Pantone SkinTone Guide) (Fig. 2A). Behavioral experiments were performed in the wind tunnel to individually test various faux skin tones (Y02, Y10, R10, and an unpleasant orange shade typical of individuals using cheap tanning lotion [which we designated "vile 45"]) using the white object as a control. Similar to the previous experiments, only during CO_2 release did mosquitoes become highly attracted to skin tones (Fig. 2C, 2E; Kruskal-Wallis test, df = 8, Chi-square = 184.37, $P < 0.001$), exhibiting no behavior characteristic of attraction before exposure to CO_2 (paired t-test, $P = 0.09$). Moreover, the mosquitoes exhibited similar levels of attraction to each skin tone (multiple comparison Kruskal-Wallis test, $P > 0.05$) (Fig. 2C, 2E).

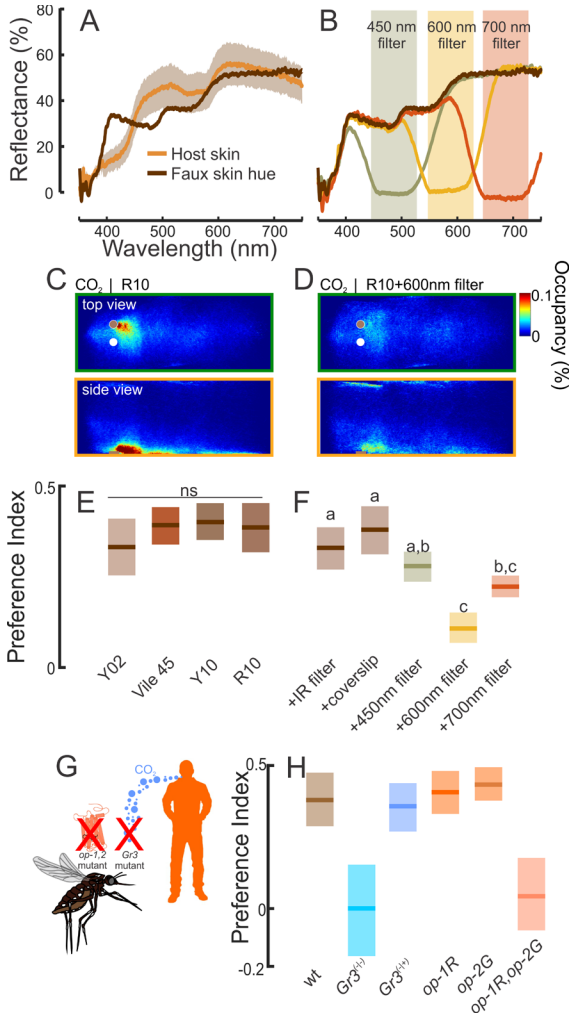

Figure 2. The contribution of orange-red wavelengths in attraction to faux human skin. (**A**) Spectral reflectance of human skin and faux skin used in behavioral experiments. (**B**) Ultra-thin optical filters (450 nm, 600 nm, and 700 nm) attenuated discrete bands in the object's reflected spectrum. (**C, D**) Occupancy maps of the mosquito's distribution around the visual objects during exposure to CO_2. During CO_2, mosquitoes were significantly attracted to the faux skin color compared to the white (control) object (C). However, the optical filter attenuating the 550-630 nm band reduced the numbers of mosquitoes investigating the faux skin color (D). (**E, F**) Mosquitoes significantly preferred the faux human skin colors (E), although optical filters in the yellow to red wavelengths significantly decreased the attractiveness of the visual object (F). Boxplots are the mean (line) with 95% confidence interval (shaded area); letters denote statistically significant differences between groups. ($n \geq 15{,}035$ mosquito trajectories for each treatment). (**G**) Testing a mosquito line deficient in long-wavelength opsins (*opsin1* and *opsin2*), or unable to detect CO_2 (*Gr3* mutant) allowed us to examine the contribution of olfactory and visual input into the attraction of human skin color. (**H**) Mean preference indices for the Gr3 mutants (blue) and opsin mutants (orange). All mosquito lines showed similar preferences to the white and skin color visual objects during exposure to filtered air (Kruskal-Wallis test: df = 3, Chi-sq = 1.68, P = 0.64). However, during CO_2 the lines were significantly different from one another in their visual preferences (Kruskal-Wallis test with multiple comparisons: df = 3, Chi-sq = 96.01, $P < 0.001$): only the heterozygote (*Gr3*$^{-/+}$) and wild-type (LVP) lines showed significant attraction to the skin color (one-sample t-test: $P < 0.001$), whereas the opsin double mutant line (*op-1/op-2*) and the *Gr3*$^{-/-}$ mutants showed no attraction (one-sample t-test: $P > 0.31$). Boxplots area the mean (line) with 95% confidence interval (shaded area) ($n \geq 3{,}277$ mosquito trajectories for each treatment).

To determine which region of the human skin visual spectrum is most attractive to mosquitoes, we overlaid the R10 skin color card with optical filters to attenuate discrete bands (Fig. 2B). Whereas the 450-nm optical filter had no significant effect on behavioral attraction to the skin tone compared with the positive controls (Fig. 2F; multiple comparison Kruskal-Wallis test, $P > 0.58$), filters blocking longer

174 wavelengths (550- to 700-nm) reduced the attractiveness of the visual object ($P < 0.05$). In particular,
175 application of the 600-nm filter was associated with a 300% reduction in attraction compared with the
176 positive controls (Fig. 2C–F). Importantly, results for controls consisting of an overlaid infrared filter or a
177 clear nylon coverslip did not differ significantly from the unmanipulated skin tone (multiple comparison
178 Kruskal-Wallis test, $P > 0.33$). To further examine the importance of visual and olfactory integration in
179 controlling mosquito visual preferences, we examined single and double mutants of the long-wavelength
180 photoreceptors *opsin-1* and *opsin-2* and a line with a mutation in the Gr3 receptor[14], which transduces
181 CO_2 signals (Fig. 2G). Whereas the *Gr3*-heterozygote, *opsin-1* and *opsin-2* single mutants, and wild-type
182 control mosquitoes were significantly attracted to the skin tone during CO_2 exposure (one-sample t-test: P
183 < 0.001), neither the *opsin-1,opsin-2* double mutant nor *Gr3* mutant were attracted to the skin tones (one-
184 sample t-test: $P > 0.31$) (Fig. 2H).

185 The behavioral preference to the long wavelengths in the skin color cards may not reflect
186 mosquito behaviors to the hues reflected from human skin. To examine this further, we tested mosquitoes
187 in a smaller opaque cage (45 cm x 30 cm x 30 cm) where they were exposed to two small windows (16
188 cm^2) (Fig. 3A,B). The cage and its environs were constructed to minimize any uncontrolled
189 contamination from thermal or olfactory cues, and the windows being made from clear, heat absorptive
190 glass (Fig. S2). The back of a hand was displayed in one window, and the back of a heat-protective white
191 glove was displayed in the other window (as a control). Similar to the assays in the wind tunnel, we found
192 that mosquitoes were highly activated by CO_2 (Fig. 3C, D, E), and this increased their visual attraction to
193 visual stimuli, including skin (Fig. 3B, C, F; Kruskal-Wallis test, df = 2, Chi-square = 84.04, $P < 0.001$).
194 Mosquitoes showed no preference during control experiments with two white gloves displayed in the
195 window, but significantly preferred skin (Fig. 3F; Kruskal-Wallis test, with multiple comparison, P <
196 0.001). However, when optical filters were placed over the window, blocking the longer wavelengths
197 (550- to 700-nm), the attraction was significantly reduced (Kruskal-Wallis test, with multiple comparison,
198 $P < 0.001$) and not significantly different from the negative control (Fig. 3F; Kruskal-Wallis test, with
199 multiple comparison, $P = 0.34$). Collectively, these results demonstrate that the long-wavelength band of
200 the visual spectrum plays an important role in determining mosquito attraction to skin color. In addition,
201 knockout of either visual or olfactory detection receptors suppresses mosquito visual attraction to long-
202 wavelength host cues.

203

204

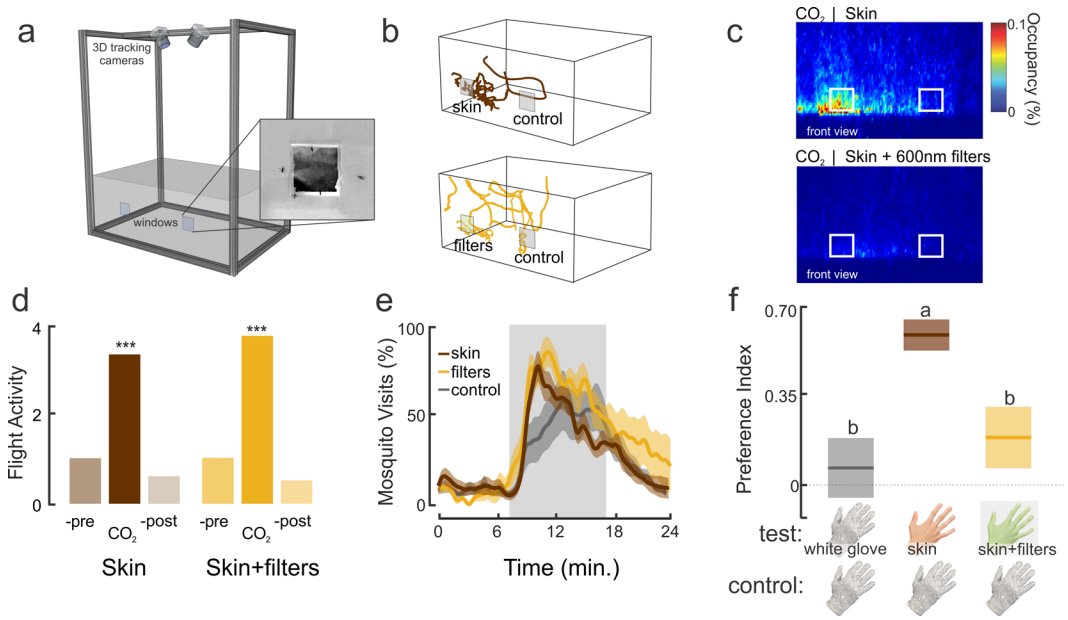

Figure 3. The importance of long wavelengths in attraction to human skin. (**A**) Cage assay with real-time tracking system, odor, and visual stimulation through two windows on the front of the cage. (**B**) Example of individual trajectories (top: skin and control (white glove), bottom: skin+filters (550-700nm) and control). (**C**) Heat maps showing the distribution of female mosquitoes during CO_2 stimulation while in presence of the skin and control (top), and the skin+filters (550-700nm) and control (bottom). (**D**) Relative flight activity between the different phases of the experiments (pre-, CO_2 and post-CO_2). There was no significant difference in the relative activity during the CO_2 phase between the skin and skin+600-nm filter treatments (Kruskal-Wallis test, df = 1, Chi-sq = 0.004, P = 0.96). (**E**) The percentage of mosquitoes visiting the windows over the duration of the experiment. Few mosquitoes investigated the windows before the CO_2 exposure. However, exposure to CO_2 significantly increased the numbers of mosquitoes visiting the windows relative to the pre-CO_2 period (Kruskal-Wallis test with multiple comparisons: df=5, Chi-sq. = 277.85, $P < 0.0001$), although during CO_2 there were no significant differences in the total number of mosquitoes investigating the windows between treatment groups (Kruskal-Wallis test with multiple comparisons: $P > 0.57$). Lines are the means and shaded areas the ±sem. (**F**) Mean preference index for the different treatment groups (white glove *vs.* white glove, skin *vs.* white glove, and skin+filter (550-700nm) *vs.* white globe). Boxplots area the mean (line) with 95% confidence interval (shaded area). Different letters denote statistically significant differences between groups (Kruskal-Wallis test with multiple comparisons, $P < 0.01$). (n = 13,597 for the skin treatment group; n = 9,502 for the for the skin+filters treatment group; and n = 9,368 for the control group).

Spectral sensitivity of the Aedes eye

The preference of mosquitoes for long wavelengths in the orange-red band motivated us to examine the sensitivity of the *Ae. aegypti* retina by recording ERGs that extracellularly measure the summed responses of retinal cells to visual stimuli (Fig. 4A). In the first series of experiments, a moving bar of differing hue (blue [peak 451 nm], green [537 nm], or red [>600 nm], all at the same intensity; 18° wide at 30°/s clockwise) was projected on a black background while conducting the ERG recordings (Fig. 4B). When the moving bar reached the mosquito's visual field, the ERG exhibited a negative response that quickly returned to baseline after the bar moved past the mosquito's field of view (Fig. 4B). A significant difference in hue-evoked responses was observed (Kruskal-Wallis test: df = 3, 40.03, $P < 0.001$), with the blue and green bars eliciting the strongest responses (Fig. 4B). Although responses to the red bar were

significantly weaker, the red hue still elicited ERG responses that were significantly higher than the baseline and those of the no-stimulus controls (Wilcoxon signed-rank test: $P < 0.001$).

To further characterize mosquito spectral sensitivity, we used a scanning monochromator to examine ERG responses across the near ultraviolet (UV) to far-red wavelength range (350–750 nm). *Ae. aegypti* exhibited the highest sensitivity to violet (410 nm, 3.2 mV) and cyan-green wavelengths (520 nm, 2.8 mV) (Fig. 4C, D). Strong ERG responses (0.47–1.27 mV) were still noted in the yellow-red wavelengths, although at >700 nm, the responses decreased to approximately 0.25 mV, which was still significantly higher than the baseline control (Wilcoxon signed-rank test, $P < 0.03$).

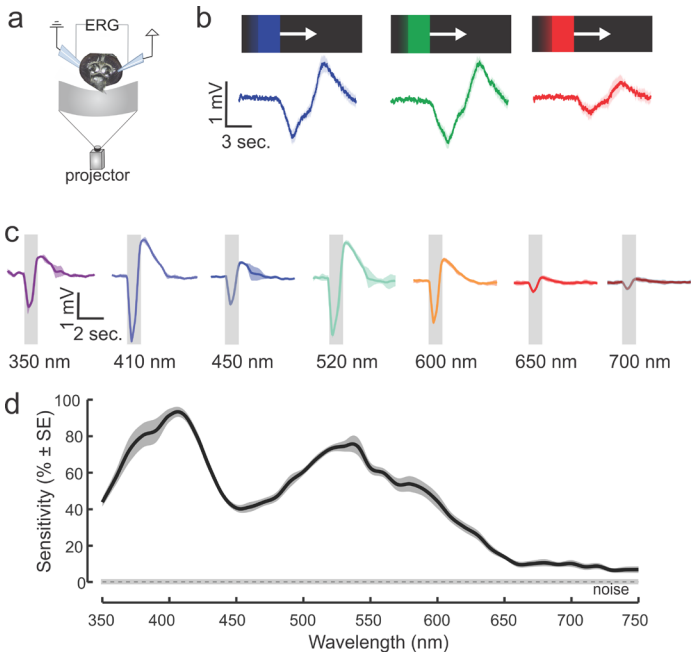

Figure 4. Retinal sensitivity to visual stimuli. (**C**) Electroretinogram responses to a blue, green or red moving bar (mean ± sem; n = 7 mosquitoes). Responses to the moving object were significantly higher than the baseline for all tested hues (blue, green or red), although blue and green bars elicited higher responses (Kruskal-Wallis test, Amplitude responses ~ color moving bar, df = 2, 40.03, $P < 0.001$, n = 7 mosquitoes). (**D**) ERG responses to pulses of light ranging from 350 to 750 nm in 10 nm intervals. Upper traces are the mean responses (shaded area is the ±sem; n = 8 mosquitoes) to discrete wavelengths showing the elevated responses to violet (410 nm) and cyan-green (520 nm) hues. (**E**) Retinal sensitivity curve across the tested wavelengths from 350 to 750 nm (10 nm intervals). Two maxima occurred at the violet (420 nm) and green (~530 nm) wavelengths, although responses were still significantly elevated above the noise at wavelengths more than 650 nm (t-test, ERG vs. noise: $P < 0.01$).

The role of visual contrast in determining mosquito preferences

Mosquitoes are very sensitive to detecting dark objects that contrast highly with the background[8,11]. In the above experiments, we kept the total object contrast (400–700 nm) with the background approximately the same, but the mosquitoes' preference for red objects and skin tones motivated us to evaluate whether these responses were due to contrast alone (calculated as the Weber contrast, or the

difference in spectral irradiance reflected by an object and the background, divided by the sum of the two) or whether mosquitoes can discriminate red-orange objects independently of intensity. As the first step in determining how features of a visual stimulus impact mosquito visual preference, grey objects that contrasted differently with the background were tested against a white control object (Fig. 5, Weber Contrasts: −0.28 to 0.02). Similar to the above results and across all tested stimuli, the presence of CO_2 increased mosquito flight activity and the number of visits to the visual objects (Fig. 5C, Wilcoxon signed-rank test, Air vs. CO_2: $P < 0.001$). Female mosquitoes exhibited significantly greater attraction to the majority of the grey visual objects than the white control object (Fig. 5D, one-sample t-test: $P < 0.001$). However, when exposed to the lightest grey object, which closely approximated the background and the white object, mosquitoes showed no preference for either object (Fig. 5D; Student's t-test: $P = 0.33$). Overall, object darkness and contrast with the lighter background was significantly related to mosquito preference, with mosquitoes investigating and preferring darker objects (Fig. 5D; Kruskal-Wallis test: df = 5, Chi-square = 634.16, $P < 0.001$). Although mosquitoes showed a distinct preference for darker objects, mosquito flight velocity and duration did not significantly differ across treatments (Kruskal Wallis test: Chi-square > 7.40, df = 5, $P > 0.055$).

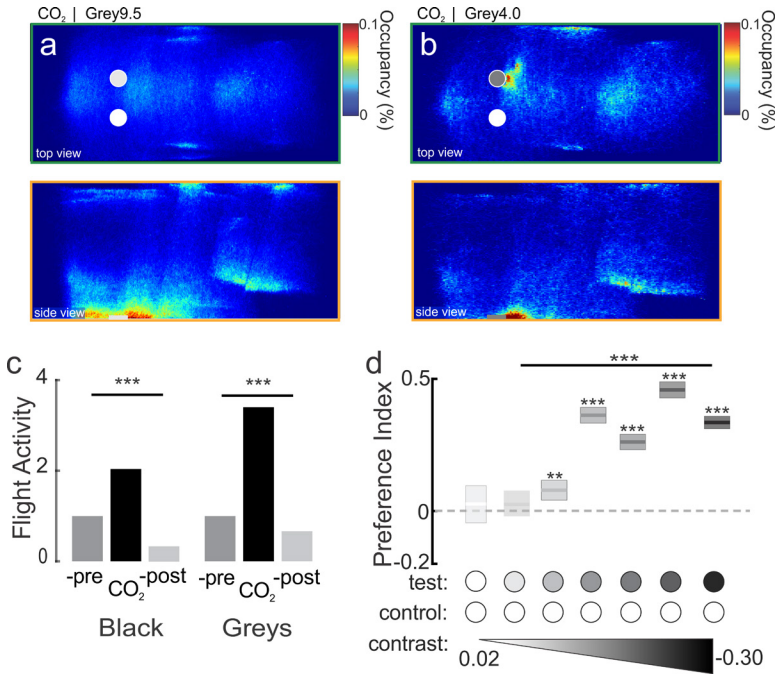

Figure 5. The effect of achromatic contrast on mosquito attraction to visual objects. (**A**) Occupancy map of the distribution of female mosquitoes during CO_2 delivery in presence of a white and a light grey object (Weber Contrast: -0.05). The top plot is the top view of the working section of the tunnel (x,y), and the bottom plot is the side view (x,z). (**B**) As in A, except the grey object has a higher contrast (-0.23). (**C**) Relative flight activity between the different phases of the experiments (pre-, +CO_2 and post-CO_2). Mosquitoes exhibited similar flight activities across all tested visual objects (Kruskal-Wallis test, df = 1, Chi-sq = 3.24, $P = 0.07$). (**D**) Mean preference index for the test (grey, or black) vs. control object (white) with 95% confidence interval ($n \geq 27{,}537$ mosquito trajectories per tested grey object). Object contrast had a significant effect on the attraction to the tested object (Kruskal-Wallis test: Preference Index ~ contrast tested object, df = 5, Chi-sq = 634.16, $P < 0.001$). All gray objects were significantly more attractive than the control, white object (one-sample t-test, **: $P < 0.01$, ***: $P < 0.001$) except for the lightest grey object (-0.05), which was not more attractive (one-sample t-test: $P = 0.33$).

279 ***Effects of contrast and color locus discrimination on Aedes preferences***

280 Given the difference between high retinal sensitivity to medium-long (green) wavelengths, lack of
281 attraction to green objects, and the relatively low ERG sensitivity to long (orange/red) wavelengths but
282 strong behavioral attraction to those objects, we asked the following question: what role does the darkness
283 of the object (i.e., its contrast) have on behavioral preferences *versus* the object's hue? Although we
284 lacked the photoreceptor tunings that would allow us to normalize the inputs between spectral channels,
285 we experimentally manipulated object contrast to equalize the perceptual contrast of the objects to the
286 mosquitoes and then examined the mosquito's ability to discriminate between different bands of the
287 visual spectrum.

288 We first performed behavioral experiments in which we altered the darkness of the grey objects
289 to determine the contrast that matched the attraction shown to the red hue (Fig. 6A, B). Across a range of
290 grey contrast levels, the red hue was significantly more attractive to the mosquitoes than the grey objects
291 (Fig. 6A, C, E) (Kruskal-Wallis test: Chi-square = 149.75, df = 6, $P < 0.0001$). As the grey objects
292 became darker, however, they became more attractive to the mosquitoes, and the strong preference for the
293 red hue decreased (Fig. 6E). The attractiveness of the red hue equaled that of the darkest grey and black
294 objects (Fig. 6E, one-sample t-test: $P = 0.07$ and $P = 0.08$ for the darkest grey [grey 1.5] and black
295 objects, respectively). We then determined which contrast of a green hue matched the attraction to the red
296 object. For this purpose, we used the darkest grey object that was equally attractive as the red hue and
297 tested it against different green objects (peak wavelength = 510 nm) that differed in terms of background
298 contrast (Fig. 6B). The dark grey object was significantly more attractive than most green objects, but the
299 darkest green object elicited the same level of attraction (preference index = −0.01; one-sample t-test: $P =$
300 0.66) (Fig. 6F).

301 To determine whether mosquitoes can discriminate between objects of different hues but similar
302 levels of apparent contrast, we tested attraction to the red hue *versus* the darkest green (Fig. 6G, H).
303 During exposure to CO_2, mosquitoes were strongly attracted to the red hue but not the dark green (Fig.
304 6G, H; one-tailed t-test: $P < 0.0001$). We also determined whether mosquitoes could discriminate between
305 closely related color loci. For this purpose, we matched the apparent contrast of the non-attractive blue
306 hue to an attractive grey and then subsequently compared mosquito responses to cyan (another attractive
307 hue) and dark blue, as well as cyan and dark green. Similar to the results observed with the red hue,
308 mosquitoes significantly preferred the cyan objects over the dark green or dark blue objects (Fig. 6H; one-
309 tailed t-test: $P < 0.0001$). Thus, mosquitoes easily discriminated between color hues even when the object
310 contrasts matched.

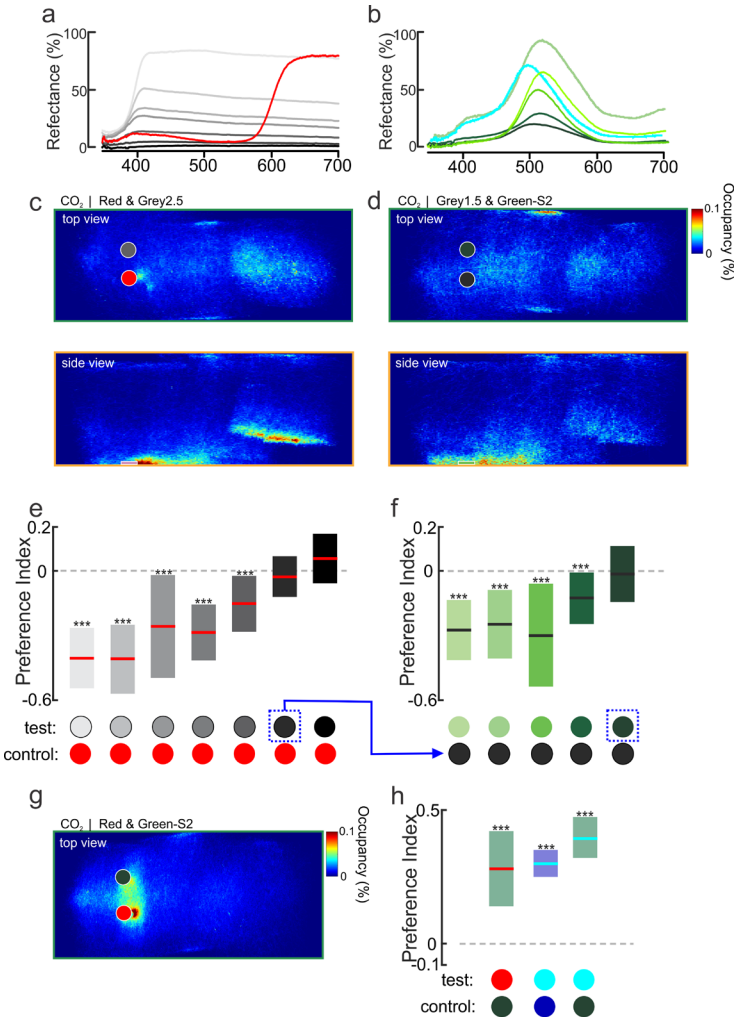

Figure 6. The role of hue *versus* contrast in mosquito visual attraction. (**A**) Spectral reflectance of red (R-Hue), black, and grey objects used in the experiments: Grey 9.5, 6.5, 4.5, 4.0, 2.5, and 1.5 , with Weber contrast values of -0.17, -0.30, -0.05, -0.10, -0.20, -0.24, -0.27, and -0.28, respectively. (**B**) Spectral reflectance of cyan and green objects used in the experiments: Gw-T1, Gw-T3, Gc-T1, Gc-Hue, G-S1, and G-S2, with Weber contrast values of -0.18, -0.11, -0.17, -0.20, -0.25, and -0.27, respectively. (**C, D**) Occupancy maps showing the distribution of female mosquitoes during CO_2 delivery in presence of the green (Gc-Hue) and white objects (C), or the red (R-Hue) and white objects (D); both the green and red have approximate similar levels of contrast with the background (Weber Contrast of -0.20 and -0.17, respectively). The upper and lower plots correspond to the top (x,y) and side (x,z) views of the wind tunnel. (**E**) Mean preference indices (±CI) for the red *versus* grey objects with different levels of contrast with the background. As the grey object's contrast increased and became darker, the relative attraction to the red object decreased, until at Grey1.5 (Weber Contrast value of -0.28) the preference was not significantly different from 0 (one-sample t-test: P = 0.07)(*n* = -17,336 trajectories for each tested object). (**F**) The Grey1.5 object was subsequently used in experiments testing the attractiveness of green objects with different levels of contrast (blue arrow from E). The grey object was significantly more attractive than the majority of the tested green objects (one-sample t-test: P < 0.001, denoted by asterisks), although the darkest green (G-S2; Weber Contrast = -0.27) was not significantly different from 0 (one-sample t-test: P = 0.66))(*n* = 10,098-15,578 trajectories for each tested object). (**G**) As in C, occupancy maps showing the distribution of trajectories around the red and dark green objects. (**H**) Mean preference indices (±CI) for red versus dark green objects, and cyan versus dark blue or dark green objects. The dark green and dark blue objects, with similar apparent contrasts to the red or cyan objects, were tested as the controls. Mosquitoes significantly preferred the red and cyan objects over the dark green or dark blue objects (one-sample t-test: P < 0.0001, denoted by asterisks). For panels E, F and H, boxplots area the mean (line) with 95% confidence interval (shaded area), and asterisks denote P < 0.001 (one-sample t-test) (n = 7,191 – 27,717 mosquito trajectories for each tested object).

By incorporating object contrasts, reflectance values, and peak wavelengths as independent variables into a series of linear models, the results of the behavioral tests offered a means to examine the

333 relative contributions of these variables toward mosquito preferences. In these models, all possible
334 combinations were tested, and the best model was selected based on its Akaike Information Criterion
335 (AIC) score, where the AIC estimates the value of each model and lower scores reflect the quality of the
336 statistical model. Using combinations of the independent variables, we found the best model (and hence,
337 lowest AIC score) relied on object contrast and wavelength, and excluded reflectance (Fig. S3A, B). But
338 which hues might be critical for mediating these behaviors? To further explore the relationship between
339 the specific wavelengths of an object's hue and its attractiveness, a series of linear models were run using
340 a multivariate analysis (PCA) of each object's visual spectrum. The PCA analysis allowed reduction of
341 highly collinear and dimensional spectral data into reduced components, which can then be used as
342 independent variables in the model. The best model explained approximately 17% of the variance in hue
343 attractiveness (Fig. S3C) and indicated that preference is negatively correlated with the content of the
344 green band (500 to 575 nm) in the object's visual spectrum (Fig. S3D, E).

345

346 ***Comparison of color preference between mosquito species***

347 The strong and specific responses of *Ae. aegypti* to hues in the visual spectrum and the similarity in long-
348 wavelength opsin gene expansion in other mosquito species[22] motivated us to examine the color
349 preferences in *Anopheles* (*An.*) *stephensi* and *Culex* (*Cx.*) *quinquefasciatus* mosquitoes. To examine the
350 color preferences in *An. stephensi* and *Cx. quinquefasciatus*, we first conducted ERG recordings of 7-day-
351 old females and examined their retinal responses to discrete wavelengths from 350 to 750 nm (Fig. 7A).
352 Both mosquito species exhibited the strongest response to UV-visible violet wavelengths (350–420 nm),
353 and the second strongest response was observed in the cyan-green wavelengths (500–520 nm). The strong
354 response of *An. stephensi* and *Cx. quinquefasciatus* to the UV wavelengths contrasted with that of *Ae.*
355 *aegypti* (dashed line), which exhibited the strongest response in the violet range (Figs. 3D and 7B,C). All
356 three species exhibited similar responses to the long wavelengths in the orange to red band (620–750 nm).

357 Are mosquito species' behavioral preferences for visual objects correlated with their ERG
358 responses, and are their color preferences similar? To answer these questions, we tested the responses of
359 *An. stephensi* and *Cx. quinquefasciatus* mosquitoes to blue, green, red, and black objects in the wind
360 tunnel using a methodology similar to that used for *Ae. aegypti*, except at lower light levels (1.28
361 $\mu W/cm^2$). As with the results for *Ae. aegypti*, exposure to CO_2 caused a doubling in the number of flying
362 mosquitoes and increased the percentage of mosquitoes that investigated the visual objects 5.58- to 9.15-
363 fold relative to air-only treatment for *An. stephensi* and *Cx. quinquefasciatus*, respectively (Kruskal-

Wallis test: df = 2, Chi-square > 7, P < 0.01) (Fig. 7D). However, in contrast to the tight clustering around attractive visual objects by *Ae. aegypti* (Fig. 1D), occupancy maps showed that the responses of *An. stephensi* and *Cx. quinquefasciatus* mosquitoes were much more diffuse (Fig. 7E, F). Nonetheless, *Cx. quinquefasciatus* formed a clustering hotspot around the outlet of the odor plume nozzle that was much stronger than the responses of the other two species (Figs. 1D; 7E, 7F). Although we tried to minimize the odor nozzle's visual signature by using clear acrylic and tubing, *Cx. quinquefasciatus* mosquitoes might have located the plume source based on the high CO_2 concentration or by seeing the nozzle to some degree.

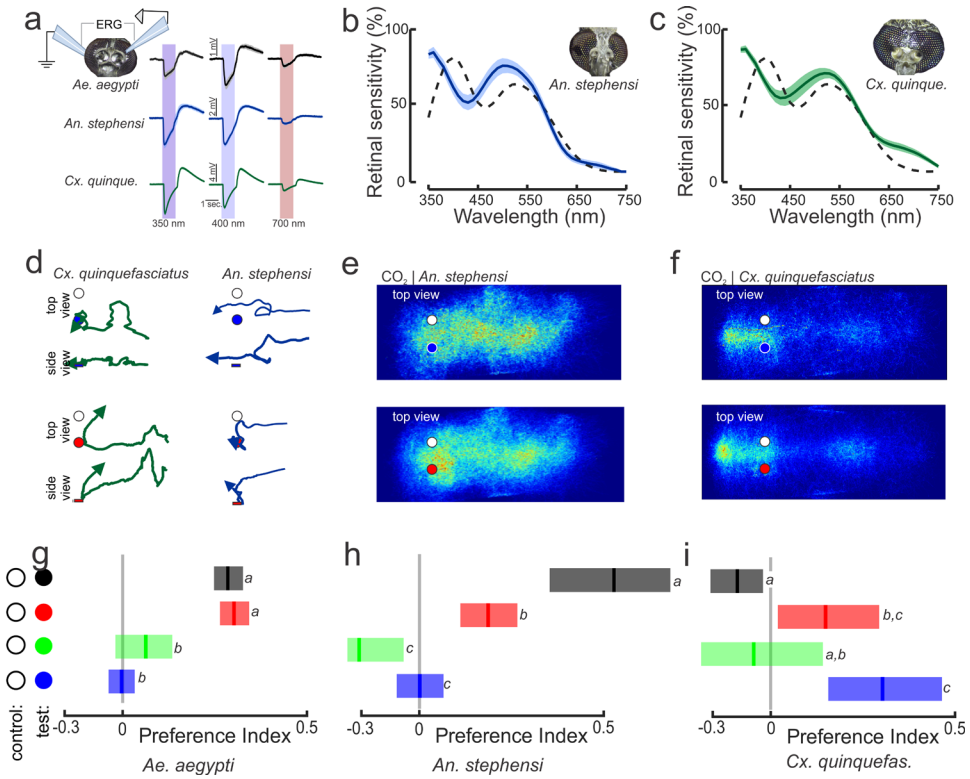

Figure 7. Species-specific responses to hues. (**A**) ERG recordings from *Ae. aegypti*, *An. stephensi* and *Cx. quinquefasciatus* mosquitoes. Traces are responses to 1-sec. pulses of light in the 350 nm, 400 nm, and 700 nm bands. Each trace is the mean ± sem of 7-9 mosquitoes/species. (**B**, **C**) Retinal sensitivity to discrete wavelengths show that both *An. stephensi* (B) and *Cx. quinquefasctiatus* (C) have the strongest responses in the UV (360 nm) and green (520 nm) bands. The dashed line is the retinal sensitivity of *Ae. aegypti*. (**D**) Representative flight trajectories [(x,y) and (x,z)] of *Cx. quinquefasciatus* (left) and *An. stephensi* (right) mosquitoes. *Cx. quinquefasciatus* showed a mild attraction to the blue object (top), whereas *An. stephensi* showed an attraction to the red object (bottom). (**E**, **F**) Occupancy maps (x,y) of *An. stephensi* (E) and *Cx. quinquefasciatus* (F) distribution around the blue (top) and red (bottom) objects during CO_2 exposure. (**G-I**) The preference indices for *Ae. aegypti* (G), *An. stephensi* (H) and *Cx. quinquefasciatus* (I) in response to the black, red (R-Hue), green (Gc-T1), and blue (Bw-T1) objects. Lines are the means and shaded bars are the confidence intervals (n > 2153 mosquito trajectories per treatment; letters denote statistical comparisons, Kruskal-Wallis test with multiple comparisons: P < 0.05).

We next examined the preferences of the mosquito species for different spectral objects (black, blue, green, or red) relative to the white object (the non-attractive control). Similar to *Ae. aegypti*, when both *An. stephensi* and *Cx. quinquefasciatus* mosquitoes were subjected to filtered air treatment, they

showed no preference for the black object or any of the spectral objects relative to the white control object (preference indices of -0.04 and 0.08 for *An. stephensi* and *Cx. quinquefasciatus*, respectively; Kruskal-Wallis test: df = 3, Chi-square < 3.66, P > 0.30). However, their spectral preferences changed when exposed to CO_2. After encountering the CO_2 plume, *An. stephensi* preferred the black and red objects (Fig. 7G, 7H) (Kruskal-Wallis test: df = 3, Chi-square = 38.6, P < 0.001), but they were not significantly attracted to the blue or green objects (Fig. 7H) (multiple comparison Kruskal-Wallis test: P > 0.05). By contrast, *Cx. quinquefasciatus* mosquitoes preferred the blue and red objects (Kruskal-Wallis test: df = 3, Chi-square = 13.6, P < 0.01; with multiple comparisons: P < 0.05) but were not significantly attracted to the green or black objects (multiple comparison Kruskal-Wallis test: P > 0.05) (Fig. 7I). Collectively, these results show that odor strongly sensitizes attraction to visual objects across mosquito species; however, spectral preferences can be species specific.

Discussion

Free-flight behavioral experiments with mosquitoes have shown that these insects integrate olfactory, visual, skin volatiles, and thermal cues to function efficiently and robustly in complex environments[11,14,28]. However, we know very little about mosquito visual-guided behaviors or how vision is involved in host selection. In this study, we utilized real-time tracking of mosquito behaviors in a large wind tunnel. The wind tunnel system enables control of aerodynamic conditions to structure the odor plume and allow the plume and visual objects to be decoupled in time and space. Both are important considerations when testing olfactory-visual integration. In this study, and similar to our previous work using achromatic objects[11,28], the presence of CO_2 increased mosquito responses to colored objects in a hue-specific manner. Both chromaticity and contrast were important components in visual object attraction and could partly explain mosquito preferences for objects that appear orange and red to human observers. These results were qualitatively similar to those reported by Smart and Brown (1957), who examined the landing responses of mosquitoes on colored cloth in a field[17]. The results of their study showed that mosquitoes (*Aedes* sp.) are attracted to red and black cloths, with darker colors being more attractive than lighter shades[17]. Our ERG results and wind tunnel assay data suggest that mosquitoes can detect and are attracted to the long wavelength bands in the orange and red portions of the human visual spectrum, although if objects contrast highly with the background and/or are darker, then they become more attractive. The demonstrated spectral preferences of mosquitoes and their lack of attraction to lighter colors, with dominant bands in the blue and green regions, impacted the fashion industry in the early twentieth century. For instance, Nuttall and Shipley (1902)[29] suggested wearing khaki pants would be appropriate for ensembles in a tropical environment, and the US military changed its dress shirts from

420 dark blue to light blue in part to mitigate mosquito biting[30]. Nonetheless, a key question is what drives
421 these responses in mosquitoes, particularly the attraction to darker and higher-contrast colors? An
422 important component could be the visual OFF responses to the visual background[31]. In our wind tunnel,
423 we projected a light grey checkerboard pattern on the bottom of the tunnel to provide optic flow and
424 contrast with the visual objects. The lack of opsins for the red hue could cause an OFF response in
425 downstream neurons that receive input from the photoreceptors. One complication with this hypothesis is
426 that mosquitoes still preferred the red hue when tested against a dark green object that matched it in
427 apparent contrast, suggesting they have an ability to detect these long wavelengths. This was further
428 demonstrated by the ERG responses to long (red) wavelengths. Recent work in *Drosophila* has shown
429 that photopigments provide a mechanism for flies to detect orange and red wavelengths[32], and it is
430 possible that similar processes play a role in mosquitoes.

431 Although the contrast with a lighter background did impact the attraction responses of *Ae. aegypti*
432 mosquitoes, the preferences for the red and cyan hues were greater than the apparent contrasts of the
433 competing visual cues (green, or blue). The *opsin-1* and *opsin-2* genes, which are tuned to the green to
434 orange band of the visual spectrum, are highly expressed in the mosquito retina. The results of this study
435 and those reported elsewhere[25] suggest that *opsin-1* and *opsin-2* play important roles in determining
436 object preference and visual attraction to human skin. Additional research will be needed to identify the
437 opsins and neural circuits involved in small-field object detection and color preference and determine how
438 odor modulates those responses.

439 Compared with other insects, such as honeybees or the tsetse fly, we know little about mosquito
440 visual ecology or how visual cues are integrated with other senses in these insects. Whereas shallow pools
441 of water can be rich in green and red wavelengths and flowers dominant in blue and green, hosts' skin is
442 dominated by long wavelengths in the green to red band of the visual spectrum (Fig. 1B). Abundant work
443 by the cosmetics industry has shown that human skin has a lower peak in the green wavelength (530 nm,
444 ~20%) and a dominant reflectance in the orange to red wavelengths (>600 nm, 20–60%). The diurnal *Ae.*
445 *aegypti* and nocturnal and crepuscular *An. stephensi* and *Cx. quinquefasciatus* mosquitoes are all active
446 during periods in which these longer wavelengths are dominant. For example, *Ae. aegypti* exhibit peak
447 activity in the mornings and late afternoons, and *An. stephensi* and *Cx. quinquefasciatus* mosquitoes are
448 especially active during moonlit nights—both environments are long-wavelength shifted[21,33,34]. In this
449 study, we show that mosquitoes are especially sensitive to long wavelengths (yellow to red) for host
450 detection; blocking these wavelengths can suppress object attraction. Moreover, we found that mosquitoes
451 can distinguish between closely colored loci (Fig. 6H), even when their apparent contrasts match. Insect
452 photoreceptors within an ommatidial cartridge transduce light intensity and spectral information. At the

453 photoreceptor terminals, they also provide antagonistic inputs to downstream neuron targets, thus
454 allowing discrimination of spectral inputs (termed 'color opponency'). In *Drosophila melanogaster*, color
455 opponency at the photoreceptor terminals plays an important role in their color discrimination and
456 preference[31], and it could be that similar processes are at play in mosquitoes. In a variety of insects,
457 including flies, bees, and butterflies, spectrally sensitive photoreceptors form connections with
458 transmedulla neurons that project into the lobula, where additional color and motion processing—
459 including color opponency—occurs[35-37].

460 It is important to note that our current experiments did not incorporate close-range cues from a
461 host, such as heat, water vapor, or skin volatiles. These cues play critical roles in controlling landing and
462 biting behaviors, and future work could determine how visual spectra are processed in tandem with these
463 other stimuli. Nonetheless, previous work has shown that visual cues can promote mosquito orientation
464 and search behaviors in combination with odor, heat, or water vapor[11,14]. The integration of multimodal
465 stimuli in driving behavioral responses raises questions regarding how the sensory systems are linked in
466 the brain. Odor stimulation increases visual responses in the object-detecting neuropil in the *Ae. aegypti*
467 lobula[28]. Neuropil in this brain region is responsive to moving objects but not wide-field motion.
468 Interestingly, whereas olfactory stimulation increases visual responses in the lobula, visual stimulation
469 does not modulate glomerular responses in the antennal lobe, the primary site for processing olfactory
470 information in the mosquito brain. Why might this occur? Mosquitoes have a relatively poor visual
471 resolution (~10°); thus, vision may not provide fine-scale information about the identity of an object.
472 Instead, an object's odor may provide information about its identity, whereas vision can provide details
473 regarding the location of the object.

474 Despite the potential importance, few studies have examined retinal responses to long
475 wavelengths in mosquitoes[23,24], and how peripheral and downstream visual circuits, such as those in the
476 optic lobes, process this information remains unknown. Evolutionary analyses of long-wavelength opsins
477 in diverse mosquito species have suggested these genes are functionally important. In *Ae. aegypti*,
478 *Anopheles coluzzii*, and *Cx. quinquefasciatus*, these genes have undergone duplication events and may be
479 under positive selection, explaining the commonalities in ERG responses. *Aedes aegypti* has 10 putative
480 opsins, five of which are potential medium- to long-wavelength opsins in the adult (>500 nm)[22]. One of
481 these genes, *opsin-1*, is expressed in the largest group of photoreceptor cells (R1-R6) in the *Ae. aegypti*
482 eye[23]. The R1-R6 photoreceptors form a trapezoid-like structure in the ommatidial cartridge, with the R7
483 and R8 cells in the middle. Perhaps similar to *D. melanogaster* with rhodopsin-1 (Rh1), the *Ae. aegypti*
484 *opsin-1* is likely involved in motion- and dim-light sensitivity[38]. The inner R7 and R8 photoreceptors are
485 involved in color vision, and the *Ae. aegypti opsin-2* is expressed in the R7 photoreceptors located in

486 distinct bands on the dorsal and ventral surfaces of the eye, and possibly used for navigation and biting
487 behaviors. For mosquitoes, opsins that differ in spectral tuning can be co-expressed in the R7
488 photoreceptor in the female retina (e.g., the long-wavelength *opsin-2* and short-wavelength *opsin-9*),
489 thereby increasing their range in wavelength sensitivity[39]. This may contrast the opsin co-expression in
490 *D. melanogaster* R7 cells in the dorsal region of the eye, where two short (UV)-sensitive opsins are co-
491 expressed[40], presumably to increase the spectral contrast with the green-absorbing opsins in the R8 layer.
492 The opsin co-expression and broadening of spectral input in mosquitoes could be advantageous under
493 low-light conditions, as photon capture would be maximized, thus allowing for detection of suitable hosts
494 or perhaps sources of nectar[39,41], but this advantage would come at the cost of detection of particular
495 wavelength bands. In our study, however, mosquitoes were able to discriminate between distinct and
496 overlapping spectral bands (green and red; cyan and green, and cyan and blue, respectively), all at the
497 same apparent contrasts, suggesting that other opsins, perhaps in the R8 cells, or downstream circuits,
498 play a role in increasing the separability of those hues.

499 Color vision plays a critical role in a diverse array of insect vectors, and it is integrally tied to
500 olfaction. For instance, traps that incorporate visual and olfactory cues have proven transformative as a
501 low-cost method for controlling tsetse flies in parts of Africa[42]. Like *Ae. aegypti*, the majority of tsetse
502 flies (e.g., *Glossina morsitans morsitans* and *G. pallidipes*) locate hosts based on smell, and once they are
503 within close range (<10 m), visual cues cause the insects to investigate and potentially bite if the object is
504 a host. Beginning with Vale (1974)[43] and continuing into the 1990s, researchers found that flies are most
505 attracted to a specific blue (approximately 460 nm), followed by red and black, but they are not attracted
506 to green and white[5,6]. Researchers subsequently found that incorporating blue and black hues in traps
507 was particularly effective at inducing flies to come into contact with insecticide-treated screens. *Triatoma*
508 *infestans* (i.e., the kissing bug) is another example of an insect that integrates odor and visual cues to
509 mediate attraction to targets. An aggregation pheromone gates the attraction of *T. infestans* to colored
510 objects, including the red, blue, and black hues, although the bugs always reject green (approximately 525
511 nm) and white hues[7]. In a similar manner, our results obtained from tests of different mosquito species
512 demonstrate the importance of olfaction in mediating mosquito color preferences. In the absence of CO_2,
513 mosquitoes did not demonstrate any preference between white and colored objects, but they became
514 attracted to specific hues in the presence of CO_2. However, there were species-specific differences in the
515 attractive hues. Whereas *Ae. aegypti* was equally attracted to both red and black objects, *An. stephensi*
516 was most attracted to black, followed by red objects. By contrast, *Cx. quinquefasciatus* was attracted to
517 blue, followed by red objects; surprisingly, however, this species was not attracted to small black objects.
518 Collectively, the results of our current study and those of other studies show that the visual systems of
519 insect disease vectors and their behaviors constitute attractive targets for the development of traps

520 incorporating visual features that can be species-specific in terms of attraction, thus providing incentive to
521 identify molecular targets that compromise mosquito olfactory-visual responses.

522

523 **Materials and Methods**

524 Mosquitoes, Odor Delivery, and Wind tunnel

525 Mosquitoes (*Aedes aegypti*, Rockefeller, Liverpool, Gr3 and Op1,Op2 mutant lines) were raised in groups
526 of 100 individuals and anesthetized with cold to sort males from females after cohabitating for 7 days. At
527 this time, more than 90% of the females have been mated, as indicated by their developing embryos. For
528 each experimental trial in the wind tunnel, we released 50 females into the wind tunnel working section 3
529 h prior to the mosquito's subjective sunset (time period of peak activity for *Ae. aegypti*). Each visual
530 stimulus was tested in 4 to 12 experimental trials (on average, approximately 5,575 trajectories were
531 quantified per trial) and 12,300 *Ae. aegypti* were flown in total across all experiments, for a total of
532 1,305,695 trajectories. After one hour, the 5% CO_2 plume (or filtered air in control experiments), was
533 automatically released from a point source at the immediate upwind section of the tunnel and at a height
534 of 20 cm and in the centerline of the tunnel. The CO_2 remained on for 1 hour, before switching off for
535 another hour of filtered air (post CO_2). The CO_2 and filtered air were automatically delivered using 2
536 mass flow controllers (MC-200SCCM-D, Alicat Scientific, Tucson, AZ) that were controlled by a Python
537 script that allowed synchronizing odor and filtered air delivery with the trajectory behaviors. The CO_2
538 plume was quantified using a Li-Cor LI-6262 CO2/H2O analyzer (Li-Cor, Lincoln, NE) for a total of 500
539 locations throughout the tunnel (Fig. 1). Data yielded an exponential decay similar to a model of turbulent
540 diffusion at the air flow (40 cm/s) and turbulent intensities (5%) of this tunnel, such that 20 cm from the
541 source and parallel to the wind flow the plume was approximately 1700 ppm (Fig. 1C, D), which is in the
542 range of the plume of human breath.

543 All behavioral experiments took place in a low-speed wind tunnel (ELD Inc., Lake City, MN),
544 with a working section of 224 cm long, 61 cm wide, by 61 cm high with a constant laminar flow of 40
545 cm/sec (Fig. 1). We used 3 short-throw projectors (LG PH450U, Englewood Cliffs, NJ) and rear
546 projection screens (SpyeDark, Spye, LLC, Minneapolis, MN) to provide a low contrast checkerboard on
547 the floor of the tunnel and grey horizons on each side of the tunnel. The intensity of ambient light from
548 the projectors was 96 lux across the 420-670 nm range. A 3D real-time tracking system[11,44] was used to
549 track the mosquitoes' trajectories. Sixteen cameras (Basler AC640gm, Exton, PA) were mounted on top
550 of the wind tunnel and recorded mosquito trajectories at 60 frames/sec. All cameras had an opaque

551 Infrared (IR) Optical Wratten Filter (Kodak 89B, Kodak, Rochester, NY) to mitigate the effect of light in
552 the tracking. IR backlights (HK-F3528IR30-X, LedLightsWorld, Bellevue, WA) were installed below and
553 the sides of the wind tunnel to provide constant illumination beyond the visual sensitivity of the
554 mosquitoes. The temperature within the wind tunnel, measured using ibuttons and FLIR cameras, was
555 22.5°C and did not show any variability within the working section[11,25]. Ambient CO_2 was constantly
556 measured outside of the tunnel and was approximately 400 ppm.

557

558 Visual Stimuli and Experimental Series in the Wind Tunnel

559 To determine the role of odor in the innate color preferences of mosquitoes, and identify the role of
560 achromatic contrast and wavelength discrminiation, a series of different experiments were conducted. In
561 each experiment, two visual stimuli, separated by 18 cm, were presented to the mosquitoes on the floor in
562 the upwind area of the tunnel and perpendicular to the direction of airflow. Visual stimuli consisted of
563 paper circles that were 3 cm diameter (Color-aid Corp., Hudson Fall, NY, USA). Reflectance spectra for
564 all the visual stimuli were characterized using an Ocean Optics USB2000 spectrophotometer with a
565 deuterium tungsten halogen light source (DH2000) calibrated with a white Spectralon standard
566 (Labsphere, North Sutton, NH, USA). The projector and working section light intensities (approximately
567 100 lux) were measured using a cosine-corrected spectrophotometer (HR-+2000, Ocean Optics, Dunedin,
568 FL, USA) 5 cm from the projector source (63 $\mu W/cm^2$). The achromatic contrasts of the visual objects
569 relative to the background were measured using the calibrated spectrophotometer and the Weber contrasts
570 calculated by the intensity of the object (I_{object}) and background ($I_{backgroun}$), where (I_{object} -
571 $I_{background}$)/$I_{background}$. In the first experimental series, we examined the innate preference of individual colors
572 relative to the non-attractive white object. Tested colors were violet, blue, cyan, green, green-yellow,
573 yellow, orange, and red (Bv-T2, Bw-, Gw-T1, Gc-, YGc-, Yw- , O- and R-Hue; Color-aid Corp.). These
574 stimuli all had similar achromatic contrasts (-0.12 to -0.18) and peak reflectance values, but had distinct
575 peak wavelengths (Fig. 1G). The position of the respective hue and white object in each replicate trial was
576 randomized.

577 In the second experimental series, experiments were performed to examine which spectral bands
578 of the human skin might attract mosquitoes. To ensure the replicability of the experiments, and enable
579 the control of visual object humidity, temperature, and odor, we first elected to first use faux skin mimics
580 (Pantone SkinTone Guide; Pantone LLC, Carlstadt, NJ 07072 USA). We tested four different skin tones
581 (R10, Y10, and Y02) and a skin tone that we named "vile 45", which matched the putrid orange color

582 from individuals who use cheap tanning lotion (PANTONE 16-1449X, Gold Flame). Similar to our
583 previous wind tunnel experiments, each individual skin tone was paired with a white control object. To
584 attenuate different spectral bands reflected from the skin tone, we used ultra-thin (~200 um thick) plastic
585 filters that were placed over the object. Filters were selected to attenuate the 450-530 nm band, the 550-
586 630 nm band, or the 650-730 nm band (36-333 [notch filter], 35-894 [long-pass filter], and 35-896 [long-
587 pass filter], respectively; Edmund Optics Inc., Barrington, NJ USA). Reflectance measurements of the
588 object with the filters showed the transmission loss was <5% for bands outside of the filtered wavelengths
589 (Fig. 2B). As a control to determine if attenuating a spectral band outside of the visual spectrum effects
590 mosquito behavior, we used an IR filter that allows transmission of 350-750 nm band of the visual
591 spectrum (14-547 [KG2], Edmund Optics Inc., Barrington, NJ USA). To control for the physical effect
592 that placing the plastic filter over the object may have had on mosquito behavior, we used plastic
593 coverslips with the same refractive index as glass (72261-22; Electron Microscopy Services, Hatfield, PA
594 USA). Experiments were also conducted with *Gr3*$^{-/-}$ mutants[14] and the *opsin-1*$^{-/-}$,*opsin-2*$^{-/-}$ double
595 mutants[25] to examine how loss of olfactory or visual detection, respectively, impacted mosquito
596 attraction to the skin color. As controls, we used heterozygote (*Gr3*$^{-/+}$), single mutants (*opsin-1*$^{-/-}$, *opsin-2*$^{-}$
597 $^{/-}$), and the wild-type (Liverpool) lines.

598 In the third series, the role of achromatic contrast, and not wavelength, on mosquito visual
599 preferences was examined. Grey circles (3 cm diameter), differing in their Weber Contrast (-0.28 to -
600 0.05) and ranging from near-black to very light grey (Greys 1.5, 2.5, 4.0, 4.5, 6.5, and 9.5; Color-aid
601 Corp., Greyset), were run in combination with a white circle (Weber Contrast of 0.02).

602 In the fourth experimental series, we examined whether the spectral preferences of the mosquito
603 while controlling for the apparent contrast of the different hues. We normalized the perceptual contrasts
604 of the visual objects by testing a range of greys of different contrasts with the background (Greys 1.5,
605 2.5, 4.0, 4.5, 6.5, and 9.5 [Weber Contrasts of -0.28 to -0.05]; Color-aid Corp., Greyset) in combination
606 with, and against, the red object (R-Hue; Weber Contrast = -0.17). Once we identified the grey object
607 that was as attractive as the red, identified by the PI that not significantly from 0 (t-test: $P > 0.05$), we
608 then tested that grey (Grey 1.5; Weber Contrast = -0.28) against a range of different green objects that had
609 the same peak wavelength (510 nm) but different Weber Contrasts, from light to dark (-0.11 to -0.27).
610 Based on the green object that elicited the same level of attraction as the dark grey (PI = 0), we then
611 tested the dark green versus the red object. Similar to experiments with the green objects, we tested the
612 dark grey (Grey 1.5; Weber Contrast = -0.28) against a range of different blue objects that had the same
613 peak wavelength (470 nm) but different Weber Contrasts, from light to dark (-0.13 to -0.28), followed by

614 testing the red object versus the dark blue, and the attractive cyan (495 nm) object versus the dark blue or
615 dark green objects with the same apparent contrast.

616

617 Visual Attraction to Skin in a Cage-Assay

618 To assay the visual attraction to the skin, acrylic cages (45 x 30 x 30 cm; McMaster-Carr; cat. #
619 8560K171) were constructed to allow for video recording and tracking from above. Thermal insulation
620 and white sheeting were wrapped around the cage's exterior to prevent any heat cues from outside of the
621 cage while providing a uniform visual environment to the interior. One side of the cage was partially
622 made from a white mesh allowing 5% CO_2 input to the cage. To conduct the visual preference assays, two
623 4 x 4 cm windows, spaced 18 cm apart, were cut into the acrylic. Windows were sealed with heat
624 absorptive glass (Schott KG2, Edmund Optics). Similar to the visual stimuli used in the wind tunnel
625 experiments, mosquitoes were tested with a white "control" in one window (white glove), and the other
626 window displaying either human skin, or human skin through long-wavelength optical filters (550-730
627 nm band; 36-333 and 35-894 filters; Edmund Optics Inc., Barrington, NJ USA). Positions of the visual
628 stimuli were randomized between experimental replicates. To test for any side preference or
629 contamination in the cage, control experiments were also conducted using two white gloves as the visual
630 stimuli in the windows. Experiments were performed in a chamber held at approximately 18 to 22.5°C,
631 and the cage was situated underneath a hood ventilation system allowing air exchange. A CO_2 Flypad
632 (Genesee Scientific; cat. # 59-119) was placed immediately adjacent to the side of the cage, and similar to
633 the wind tunnel experiments, CO_2 was controlled by two mass flow controllers (MC-200SCCM-D, Alicat
634 Scientific, Tucson, AZ) via a Python script that allowed synchronizing odor and filtered air delivery with
635 the trajectory behaviors. Filtered air was released for the first 8 minutes of each experiment, followed by
636 the release of 5% CO_2 for 8 minutes, before switching off for another 8 minutes (post CO2). Two cameras
637 (Basler AC640gm, Exton, PA) were mounted above the cage and recorded mosquito trajectories at 100
638 frames/sec. IR backlights (HK-F3528IR30-X, LedLightsWorld, Bellevue, WA) were installed above the
639 cage. Human skin reflectance measurements and assays were from 3 males and 3 female wild type
640 individuals on the University of Washington (Seattle) campus (ages 25-46 years old). Volunteers were
641 from various backgrounds: Hispanic (one male), white (one male and one female), and Asian (one male
642 and two females). Protocols were reviewed and approved by the University of Washington Institutional
643 Review Board, and all human volunteers gave their informed consent to participate in the research. As the
644 wind tunnel experiments, we used 6—8 day-old, non-blood-fed, mated females who were sucrose
645 deprived for 24 hours but had access to water. We released 50 females into the cage for each experiment,

646 and the assays were initiated 3 hr before lights off (ZT12). Ambient CO_2 was constantly measured both
647 inside and outside of the cage.

648

649

650 Visual preferences in *Cx. quinquefasciatus* and *An. stephensi*:

651 *Anopheles stephensi* (Indian strain) and *Culex quinquefasciatus* mosquitoes were separately raised in
652 groups of 100 individuals and anesthetized with CO_2 to sort males from females after cohabitating for 7
653 days. At the time of their subjective sunset, groups of 50 female mosquitoes were released into the
654 working section of the wind tunnel. After 1 h of filtered air, 5% CO_2 was released from a point source at
655 the upwind section of the tunnel (height of 20 cm, and in the center of the tunnel) for 1 h, after which
656 filtered air was released from the point source. The intensity of ambient light from the projectors was
657 approximately 1.3 $\mu W/cm^2$. The low light intensity, relative to that used with *Ae. aegypti*, was necessary
658 to recruit females to the visual objects. At higher light intensities *An. stephensi* and *Cx. quinquefasciatus*
659 mosquitoes responded to the CO_2 plume but they did not respond to the visual objects. We found that
660 these two species began to investigate the visual objects only at light intensities <5 lux. Like our
661 experiments with *Ae. aegypti*, the temperature within the wind tunnel was approximately 22.5°C.

662

663 Trajectories analysis:

664 Our tracking system is unable to maintain mosquito identities for extended periods of time, but we
665 considered individual trajectories as independent for the sake of statistical analysis. Analyses were
666 restricted to trajectories that were at least 90 frames (1.5 seconds) long. Only trajectories that lasted for
667 more than 1.5 seconds were analyzed (average length trajectory: 3.1 sec., longest trajectory: 96.4 sec.,
668 total number of 1,305,695). To examine the mosquito behaviors and preferences to the two visual stimuli
669 in the tunnel, a fictive volume was created around the visual cues (area: 14x14 cm, height: 4 cm). The
670 volume was centered over the object in the crosswind direction, and shifted slightly downwind in the
671 wind line direction. This volume was chosen as it captures the area of primary activity of the mosquitoes.
672 A sensitivity analysis was performed by adjusting the volume size and demonstrated that this volume best
673 captured the mosquitoes investigating the visual objects while excluding mosquitoes transiting to other
674 areas of the working section.

675 Occupancy maps were calculated by dividing the wind tunnel into 0.3-cm^2 squares. For each
676 replicate experiment, the number of mosquito occurrences within each square was summed and divided
677 by the total number of occurrences in all squares to yield a percentage of residency. We did not quantify
678 landings on the spots due to limitations of the camera angles needed to identify landings. During the
679 filtered "air" treatment, mosquitoes often investigated certain areas of the working section, such as the top
680 or corners of the working section, causing hot spots in the occupancy maps. This is typical for mosquito
681 activity without a stimulus. By contrast, when CO_2 is released, these hot spots are no longer apparent, and
682 instead, the mosquitoes investigate the visual objects or navigate to the odor source, as demonstrated by a
683 hot spot in the central area of the working section or near the odor source. For each mosquito line, the
684 replicate trials were pooled to create a occupancy heatmap for the tested visual stimulus.

685 To calculate the fractions of trajectories that approached either visual object, for each trajectory
686 we calculated a preference index by determining the amount of time a trajectory spent in each volume
687 divided by the total time it spent in both volumes. If the trajectory spent all of its time in only one volume
688 then it was assigned a preference index of 1 (test object) or -1 (white neutral object). Approximately 25 to
689 50% of the trajectories approached either object. From these preference indices, we calculated the global
690 mean, and bootstrapped the 95% confidence interval of the mean through random resampling of the
691 individual trajectories 500 times. In order to determine whether the mosquitoes preferred the visual
692 objects compared to elsewhere in the tunnel, we calculated the preference index for each trajectory at
693 each time point as the amount of time the mosquito spent in a particular 4x14x14 cm volume that was
694 randomly selected in the tunnel and compared them to the volumes containing the visual objects. Mean
695 flight velocities were calculated from the 3D tracks of each individual trajectory. To further examine
696 whether mosquito responses to the visual objects changed throughout the experiment, the percent of time
697 (per each minute interval) the mosquitoes investigated the visual objects was calculated. Statistically
698 significant groups were estimated using a Kruskal-Wallis, Mann-Whitney *U*-test with Bonferroni
699 correction at a P = 0.01 level, or the one-sample t-test. All recorded data were analyzed using Matlab
700 (Mathworks, 2019a release).

701

702 <u>Electroretinogram (ERG) recordings</u>

703 ERG recordings were performed by fixing 6 day-old, non-blood-fed female mosquitoes to a coverslip
704 using Bondic glue. Mosquitoes were dark-adapted for 1 h prior to stimulation. The recording glass
705 electrode (thin-wall glass capillaries; OD, 1.0 mm; length, 76 mm; World Precision Instruments, cat. #

706 TW100F-3) was pulled using a micropipette puller (Sutter Instrument, p-2000), and filled with Ringer's
707 solution (3 mM $CaCl_2$, 182 mM KCl, 46 mM NaCl, 10 mM Tris pH 7.2). The reference electrode, a
708 sharpened tungsten wire, was placed into one compound eye in a small drop of electrode gel (Parker, cat.
709 # 17-05), and the recording electrode was placed immediately on the surface of the contralateral eye. Two
710 different types of visual stimuli were presented to the mosquitoes. In the first series, the mosquitoes were
711 placed at the center of a semi-cylindrical visual arena (frosted mylar, 10 cm diameter, 10 cm high); a
712 video projector (Acer K132 WXGA DLP LED Projector, 600 Lumens) positioned in front of the arena
713 projected the visual stimuli. To test the response to moving objects, similar to what the mosquito might
714 encounter in flight, we tested responses to a 19° wide bar moving from left to right (Clockwise) (Fig. 4).
715 The mosquito was randomly tested with blue, green, and red bars (distinct peaks at 455, 547 nm, and 633
716 nm, 18 lux), and each colored bar was tested 10-30 times per mosquito (n = 7 mosquitoes).

717 The second stimulation method used a digital monochromator to examine responses to different
718 wavelengths across the mosquito visual spectra (350-750 nm). Mosquitoes were exposed to a 1-sec pulses
719 of light (10 lux) from a light source (35-watt Halogen; ThorLabs) and a fiber optic scanning
720 monochromator (MonoScan 2000, Mikropak GmbH, Ostfildern, Germany) that provided control of the
721 transmitted wavelengths (+/- 2 nm). Light was transmitted via optical fibers (QP600-1-SR-B X, Ocean
722 Optics, FL 32792, USA) and through a neutral density filter (fused silica, Thorlabs Inc., 0-1 OD). Each
723 mosquito preparation was tested to wavelengths of 350-750 nm in 10 nm increments (n=8
724 mosquitoes/species). The visual stimuli were calibrated using a cosine-corrected spectrophotometer (HR-
725 +2000, Ocean Optics, Dunedin, FL, USA) that was placed immediate to the recording preparation,
726 allowing us to scale the irradiance of the tested stimuli. The light-induced responses were amplified by
727 using an A-M Systems amplifier (10-100x; A-M Systems, 1800) and digitized using a Digidata data
728 acquisition system (Digidata 1550B, Molecular Devices, San Jose, CA 95134). Data were visualized and
729 analyzed using Matlab software (Mathworks).

730

731 Linear Models

732 Linear models were created using R 4.0.3 and the lm function with the default option. Comparison
733 between models were performed using the AIC function that calculates the Aikaike's Information
734 Criterion (AIC) for each model. For the first series of models, the dataset consisted of the mean
735 preference index per experiment, the contrast value, peak wavelength and brightness value for the tested
736 object. For the second series of models, the dataset contained the mean preference index per experiment

and the area under the curve (AUC) of the reflectance measurement for the tested object calculated with bins of 25 nm from 350 to 675 nm. A Principal Component Analysis (PCA) was applied to the AUC vector to remove collinearity in the object's spectrum.

Data Availability

Data on the behavioral and electroretinogram experiments can be found on Mendeley Data. Software is available on https://github.com/riffelllab.

References

1. Briscoe, A.D. and L. Chittka, *The evolution of color vision in insects.* Annual review of entomology, 2001. **46**(1): p. 471-510.
2. Hannah, L., A.G. Dyer, J.E. Garcia, A. Dorin, and M. Burd, *Psychophysics of the hoverfly: categorical or continuous color discrimination?* Current zoology, 2019. **65**(4): p. 483-492.
3. van der Kooi, C.J., D.G. Stavenga, K. Arikawa, G. Belušič, and A. Kelber, *Evolution of insect color vision: From spectral sensitivity to visual ecology.* Annual Review of Entomology, 2021. **66**.
4. Clements, A.N., *The biology of mosquitoes. Volume 2: sensory reception and behaviour*. 1999: CABI publishing.
5. Green, C., *Effects of colours and synthetic odours on the attraction of Glossina pallidipes and G. morsitans morsitans to traps and screens.* Physiological Entomology, 1986. **11**(4): p. 411-421.
6. Torr, S. and G. Vale, *Know your foe: lessons from the analysis of tsetse fly behaviour.* Trends in Parasitology, 2015. **31**(3): p. 95-99.
7. Reisenman, C.E., A.N. Lorenzo Figueiras, M. Giurfa, and C.R. Lazzari, *Interaction of visual and olfactory cues in the aggregation behaviour of the haematophagous bug Triatoma infestans.* Journal of Comparative Physiology A, 2000. **186**(10): p. 961-968.
8. Bidlingmayer, W.L. and D.G. Hem, *Mosquito (Dipteral Culicidae) flight behaviour near conspicuous objects.* Bulletin of Entomological Research, 2009. **69**(4): p. 691-700.
9. Kennedy, J.S., *The visual responses of flying mosquitoes.* Proceedings of the Zoological Society of London, A, 1939. **109**: p. 221-242.
10. WL, B., *How mosquitoes see traps: role of visual responses.* Journal of the American Mosquito Control Association, 1994. **10**: p. 272.
11. van Breugel, F., J.A. Riffell, A. Fairhall, and M.H. Dickinson, *Mosquitoes use vision to associate odor plumes with thermal targets.* Current Biology, 2015. **25**(16): p. 2123-2129.
12. Kline, D.L. and G.F. Lemire, *Field evaluation of heat as an added attractant to traps baited with carbon dioxide and octenol for Aedes taeniorhynchus.* Journal of the American Mosquito Control Association-Mosquito News, 1995. **11**(4): p. 454-456.
13. Lacey, E. and R. Cardé, *Activation, orientation and landing of female Culex quinquefasciatus in response to carbon dioxide and odour from human feet: 3-D flight analysis in a wind tunnel.* Medical and Veterinary Entomology, 2011. **25**(1): p. 94-103.

775 14. McMeniman, C.J., R.A. Corfas, B.J. Matthews, S.A. Ritchie, and L.B. Vosshall, *Multimodal*
776 *integration of carbon dioxide and other sensory cues drives mosquito attraction to humans.* Cell,
777 2014. **156**(5): p. 1060-1071.

778 15. Fay, R. and W. Prince, *A trap based on visual responses of adult mosquitoes.* . Journal of the
779 American Mosquito Control Association-Mosquito News, 1968. **28**(1): p. 1-7.

780 16. Muir, L.E., B.H. Kay, and M.J. Thorne, *Aedes aegypti (Diptera: Culicidae) vision: response to*
781 *stimuli from the optical environment.* Journal of Medical Entomology, 1992. **29**(3): p. 445-450.

782 17. MR, S. and B. AWA, *Studies on the responses of the female Aedes mosquito. Part VII—the effect*
783 *of skin temperature, hue and moisture on the attractiveness of the human hand.* Bulletin of
784 Entomological Research, 1957. **47**: p. 89.

785 18. Snow, W., *The spectral sensitivity of Aedes aegypti (L.) at oviposition.* Bulletin of Entomological
786 Research, 1971. **60**(4): p. 683-696.

787 19. Brett, G., *On the relative attractiveness to Aedes aegypti of certain coloured cloths.* Transactions
788 of the Royal Society of Tropical Medicine and Hygiene, 1938. **32**(1): p. 113-124.

789 20. Muir, L.E., M.J. Thorne, and B.H. Kay, *Aedes aegypti (Diptera: Culicidae) vision: spectral*
790 *sensitivity and other perceptual parameters of the female eye.* Journal of Medical Entomology,
791 1992. **29**(2): p. 278-281.

792 21. Trpis, M., McClelland, G. A., Gillett, J. D., Teesdale, C. and T.R. Rao. *Diel periodicity in the*
793 *landing of* Aedes aegypti *on man*. Bulletin of the World Health Organization, 1973. **48**, 623-629.

794 22. Giraldo-Calderón, G.I., M.J. Zanis, and C.A. Hill, *Retention of duplicated long-wavelength*
795 *opsins in mosquito lineages by positive selection and differential expression.* BMC Evolutionary
796 Biology, 2017. **17**(1): p. 84.

797 23. Hu, X., J.H. England, A.C. Lani, J.J. Tung, N.J. Ward, S.M. Adams, K.A. Barber, M.A. Whaley,
798 and J.E. O'Tousa, *Patterned rhodopsin expression in R7 photoreceptors of mosquito retina:*
799 *Implications for species-specific behavior.* Journal of Comparative Neurology, 2009. **516**(4): p.
800 334-342.

801 24. Hu, X., M.A. Whaley, M.M. Stein, B.E. Mitchell, and J.E. O'Tousa, *Coexpression of spectrally*
802 *distinct rhodopsins in Aedes aegypti R7 photoreceptors.* PloS one, 2011. **6**(8): p. e23121.

803 25. Zhan, Y., D. Alonso San Alberto, C. Rusch, J. Riffell, and C. Montell, *Aedes aegypti vision-*
804 *guided target recognition behavior requires two redundant rhodopsins.* BioRxiv, 2020: p. 1-30.

805 26. Angelopoulou, E., 1999. *The reflectance spectrum of human skin*. Technical Reports (CIS),
806 p.584.

807 27. Lacey, E.S., A. Ray, and R.T. Carde, *Close encounters: contributions of carbon dioxide and*
808 *human skin odour to finding and landing on a host in Aedes aegypti.* Physiological Entomology,
809 2014. **39**(1): p. 60-68.

810 28. Vinauger, C., F. Van Breugel, L.T. Locke, K.K. Tobin, M.H. Dickinson, A.L. Fairhall, O.S.
811 Akbari, and J.A. Riffell, *Visual-olfactory integration in the human disease vector mosquito Aedes*
812 *aegypti.* Current Biology, 2019. **29**(15): p. 2509-2516. e5.

813 29. Nuttall, G.H. and A.E. Shipley, *Studies in relation to malaria. II.(Cont.) The structure and*
814 *biology of Anopheles (Anopheles maculipennis).* Epidemiology & Infection, 1902. **2**(1): p. 58-84.

815 30. Packard, A., *Color-preference in insects.* Journal of the New York Entomological Society, 1903.
816 **11**(3): p. 132-137.

817 31. Schnaitmann, C., M. Pagni, and D.F. Reiff, *Color vision in insects: insights from Drosophila.*
818 Journal of Comparative Physiology A, 2020. **206**(2), p.183-198.

32. Sharkey, C.R., J. Blanco, M.M. Leibowitz, D. Pinto-Benito, and T.J. Wardill, *The spectral sensitivity of Drosophila photoreceptors.* Scientific Reports, 2020. **10**(1), p.1-13.

33. Day, J.F., *Host-seeking strategies of mosquito disease vectors.* Journal of the American Mosquito Control Association, 2005. **21**(sp1): p. 17-22.

34. Silver, J.B., *Designing a Mosquito Sampling Programme.* Mosquito Ecology: Field Sampling Methods, 2008: p. 1-23.

35. Paulk, A.C., J. Phillips-Portillo, A.M. Dacks, J.-M. Fellous, and W. Gronenberg, *The processing of color, motion, and stimulus timing are anatomically segregated in the bumblebee brain.* Journal of Neuroscience, 2008. **28**(25): p. 6319-6332.

36. Swihart, S., *The neural basis of colour vision in the butterfly, Heliconius erato.* Journal of Insect Physiology, 1972. **18**(5): p. 1015-1025.

37. Yonekura, T., J. Yamauchi, T. Morimoto, and Y. Seki, *Spectral response properties of higher visual neurons in Drosophila melanogaster.* Journal of Comparative Physiology A, 2020. **206**(2): p. 217-232.

38. Leming, M.T., *Light-dark and circadian effects on the visual response of Aedes aegypti*. 2015: University of Notre Dame.

39. Hu, X., M.T. Leming, M.A. Whaley, and J.E. O'Tousa, *Rhodopsin coexpression in UV photoreceptors of Aedes aegypti and Anopheles gambiae mosquitoes.* Journal of Experimental Biology, 2014. **217**(6): p. 1003-1008.

40. Mazzoni, E.O., Celik, A., Wernet, M.F., Vasiliauskas, D., Johnston, R.J., Cook, T.A., Pichaud, F., and C. Desplan. Iroquois complex genes induce co-expression of rhodopsins in Drosophila. PLoS biology, 2008 **6**(4): e97.

41. Peach, D.A., E. Ko, A.J. Blake, and G. Gries, *Ultraviolet inflorescence cues enhance attractiveness of inflorescence odour to Culex pipiens mosquitoes.* PloS one, 2019. **14**(6): p. e0217484.

42. Shaw, A.P., I. Tirados, C.T. Mangwiro, J. Esterhuizen, M.J. Lehane, S.J. Torr, and V. Kovacic, *Costs of using "tiny targets" to control Glossina fuscipes fuscipes, a vector of gambiense sleeping sickness in Arua District of Uganda.* PLoS Neglected Tropical Disease, 2015. **9**(3): p. e0003624.

43. Vale, G., *The responses of tsetse flies (Diptera, Glossinidae) to mobile and stationary baits.* Bulletin of Entomological research, 1974. **64**(4): p. 545-588.

44. Stowers, J.R., M. Hofbauer, R. Bastien, J. Griessner, P. Higgins, S. Farooqui, R.M. Fischer, K. Nowikovsky, W. Haubensak, and I.D. Couzin, *Virtual reality for freely moving animals.* Nature methods, 2017. **14**(10): p. 995-1002.

Acknowledgements

We are grateful for the advice and discussions with C.E. Reisenman and F. Van Breugel. Support for this project was funded by Air Force Office of Scientific Research under grants FA9550-20-1-0422 (J.A.R.); the National Institutes of Health under grants R01-AI148300 (J.A.R.), R21-AI137947 (J.A.R.); and an Endowed Professorship for Excellence in Biology (J.A.R.). C.M. was supported by a grant (EY008117) from the NEI and from the U.S. Army Research Office and accomplished under cooperative agreement W911NF-19-2-0026 for the Institute for Collaborative Biotechnologies.

Author contributions

D.A.S.A., C.R., and J.A.R. designed research; D.A.S.A., C.R., and J.A.R. performed wind tunnel experiments; C.R. and J.A.R. conducted electroretinogram experiments; A.D.S. assisted in visual stimulus, wind tunnel software, and experimental designs; Y.Z. and C.M. generated the opsin mutant lines. All authors wrote and edited the paper.

Competing Interests

The authors declare no competing interests.

Supplementary Information Figures and Legends

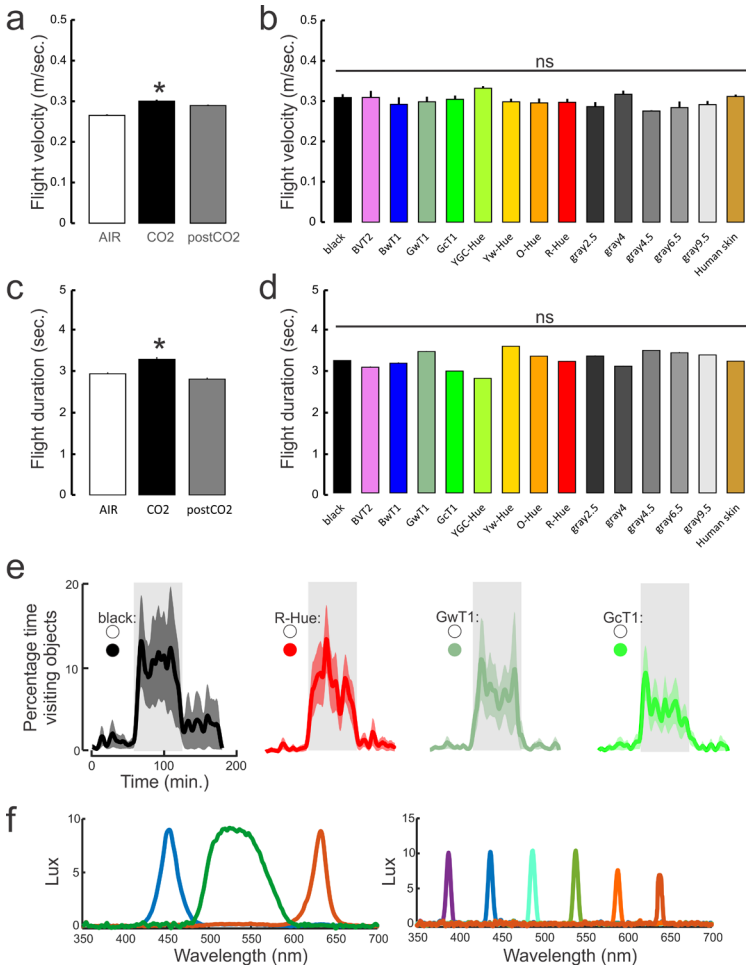

Figure S1. Flight behaviors to different color stimuli, and characterization of stimuli in ERG experiments. (A) Flight velocities of mosquitoes in different CO_2 exposure treatments (AIR-, +CO_2, and post-CO_2), across all color stimuli. Exposure to CO_2 significantly elevated the flight velocities of mosquitoes (Kruskal-Wallis test with multiple comparisons: df=2, Chi-sq. = 597.23, $P < 0.001$), although there was no significant difference between AIR and post-CO_2 treatments (Kruskal-Wallis test with multiple comparisons: $P>0.05$). Bars are the mean ± sem. (**B**) The flight velocities for each tested hue. There was no significant difference between hue treatment groups (Kruskal-Wallis test: df=11, Chi-sq. = 10.17, $P = 0.42$). Bars are the mean ± sem. (**C**) As in A, except for the mosquito flight durations. Exposure to CO_2 significantly the duration of the flight trajectories (Kruskal-Wallis test with multiple comparisons: df=2, Chi-sq. = 87.83, $P < 0.001$), although there was no significant difference between AIR and post-CO_2 treatments (Kruskal-Wallis test with multiple comparisons: $P>0.05$). (**D**) As in B, except for the flight durations of each color stimulus. There was no significant difference between hue treatment groups (Kruskal-Wallis test: df=11, Chi-sq. = 16.82, $P = 0.16$). (**E**) The number of mosquitoes visiting the

visual objects over the duration of the experiment. Few mosquitoes investigated the visual objects before or after the CO_2 exposure (Air and post-CO_2, respectively), and there was no significant difference between those two time periods (Kruskal-Wallis test with multiple comparisons between AIR and post-CO_2: $P > 0.98$). However, exposure to CO_2 significantly increased the numbers of mosquitoes visiting the visual objects (Kruskal-Wallis test with multiple comparisons: df=11, Chi-sq. = 258.72, $P < 0.001$; $P < 0.001$). During CO_2, there were no significant differences in the number of mosquitoes investigating the different hues (Kruskal-Wallis test with multiple comparisons: $P > 0.99$). Lines are the means and shaded areas the ±sem. (**F**) The lux measurements of stimuli used in the ERG experiments. Experiments used either a short-throw projector (left) or a digital monochromator (right).

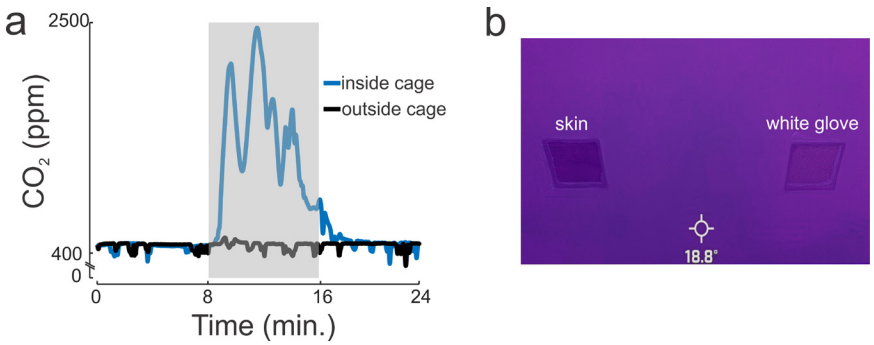

Figure S2. CO_2 and temperature measurements in the cage assay. (A) CO_2 measurements were taken outside (black trace) and inside (blue trace) the cage during experiments to measure if background contamination was occurring. CO_2 concentrations only increased in the cage during pre-programmed release from the mass flow controllers (grey shaded area). (**B**) Image taken from a FLIR camera (FLIR One Pro, FLIR Systems Inc., Goleta, CA USA) showed a constant temperature range, and did not show any variability including the region of the cage where the volunteers skin was displayed through the window. The thermal shielding and IR absorptive windows in the cage prevented a radiant heat signature that is attractive mosquitoes.

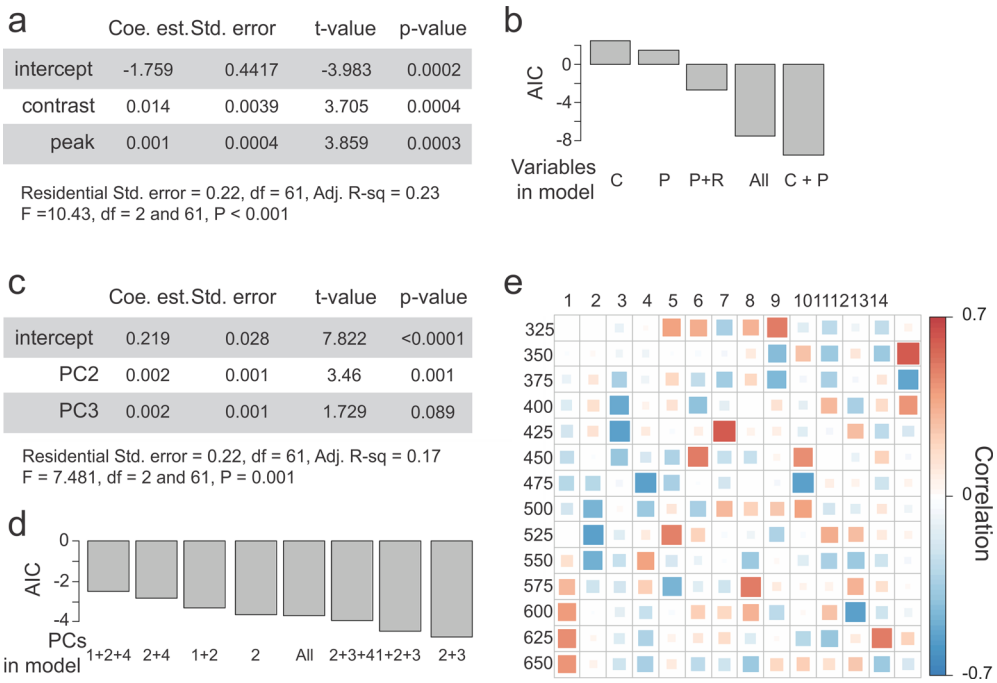

Figure S3. Models on the contributions of contrast and hue wavelength on mosquito preferences. (**A**) Linear model results based on contrast and peak wavelength values. (**B**) AIC of all the models significantly different from a null model and based on combinations of the contrast (C), peak wavelength (P) and brightness (R) values. The model in (A) was selected as the best having the lowest AIC values. (**C**) Linear regression parameters, standard errors, t-values and P-values for the model based on the PC2 and PC3. The PCs were obtained from the area-under-the-curve (AUC) of the reflectance curves calculated every 25 nm from 325 to 675 nm. (**D**) AIC of all the models significantly different from a null model and based on combinations of the first 4 PCs (representing more than 99% of the variance of the original dataset). The model in (C) was selected as the best having the lowest AIC values. (**E**) Correlation matrix between the AUC values from 325 to 675 nm and the 14 resulting PCs. The first three PCs correlated with different parts of the spectrum: PC1 was strongly positively correlated with the 575-675 nm range whereas PC2 and PC2 strongly negatively correlated with the 475-575 nm and 375-475 nm range respectively.